Stereochemistry triggered differential cell behaviours on chiral polymer surfaces†

Xing Wang,‡[ac] Hui Gan,‡[ad] Taolei Sun,*[ac] Baolian Su,[a] Harald Fuchs,[c] Dietmar Vestweber[b] and Stefan Butz[b]

Received 24th March 2010, Accepted 12th May 2010
DOI: 10.1039/c0sm00151a

One of the distinct biochemical signatures of life is the high chiral preference of biomolecules that compose the organisms, *e.g.* L-amino acids, D-sugars, L-phospholipids. As a result, many biological and physiological processes are greatly influenced by the chirality of biomolecules. This inspires the introduction of chiral effects into biomaterials research. For this purpose, we developed a novel chiral polymer brush film system containing amino acid units and report that the stereochemistry of the polymer films significantly influences the cell/substrate interaction. With two adhesive cell lines—COS-7 and bEnd.3 as examples, here we report a study of differential cell behaviors on chiral polymer film. We show that the cells can adhere, grow, spread, and assemble much better on the L-amino acid based polymer film than on the corresponding D film, although their chemical and other physical properties are all the same, indicating that the L configuration of the polymer film has better cytocompatibility than the D configuration. It not only implies a novel strategy for the design of new generation of biomaterials and devices based on the chiral effect, but may also add important knowledge to the understanding the origin of chiral preference in biosystems.

Introduction

The interaction between cells and artificial materials at the interface is an important aspect determining their biomedical and bioengineering applications.[1,2] It is not only regulated by extracellular matrix (ECM) proteins,[3] but also governed by surface chemical and physical properties of materials,[4–7] if cells are exposed to artificial surfaces. Life is a typical chiral system with characteristics of high chiral preference of biomolecules that compose the organisms,[8,9] which greatly influences many biological and physiological processes.[10] For example, chiral molecules may have different odors, and when being used in medicine, may exhibit much different or even opposite medical effects. This inspires the introduction of chiral effects into biomaterial research.

However, although it is of great importance in various domains from biomaterials to origin-of-life research, the interaction between bio-entities and chiral surfaces[11,12] has rarely been studied. As one of the few studies in this aspect, we recently reported the primary results of the specific adhesion and activation of immune cells on self-assembly *N*-isobutyryl-L(D)-cysteine monolayers on gold substrates.[12] Nevertheless, this study is only a starting point, and in order to learn more about the cellular responses to chiral surfaces, it is essential to extend this study by analyzing different kinds of chiral systems and various distinct cell types. Furthermore, it is difficult to go further using the surface model of chiral self-assembly monolayers, due to the very thin film thickness that greatly limits their practical applications and gives a relatively weak chiral characteristic to the surface. With these considerations, and to guide the effect into practical applications, we developed a novel chiral polymer brush film system, because polymers[13–15] are the mostly common-used biomaterials and the polymer brushes[16–18] show extra advantages of the easy tailorability of chemical compositions and functions and the precisely controlled surface properties with considerable bio-related applications, *e.g.* bioseparation, *anti*-biofouling, scaffolds for bioengineering,[19] *etc*. With the use of two adhesive cell lines, here we demonstrate the influence of chirality on cell behaviors on polymer surfaces. We show that the cells can adhere, grow, spread, and assemble much better on the L-amino acid based polymer film than on the corresponding D film, although their chemical and other physical properties are all the same, indicating that the L configuration of the polymer film has better cytocompatibility than the D configuration. It not only implies a novel strategy for the design of a new generation of biomaterials and devices[20] based on the chiral effect, but may also add important insights into the understanding of the origin of chiral preference in biosystems.

Results and discussions

As one of the important fundamental materials in life, most amino acids exist as L-isomers in nature, and the chirality of amino acids determines the steric configurations and conformations of proteins and other biomacromolecules,[21] thus greatly

[a]*State Key Lab of Advanced Technology for Materials Synthesis and Processing, Wuhan University of Technology, Wuhan, 430070, China. E-mail: suntaolei@iccas.ac.cn; Fax: (+86)27-8787948*
[b]*Max-Planck-Institute for Molecular Biomedicine, D-48149 Muenster, Germany*
[c]*Physics Institute, WWU Muenster, D-48149 Muenster, Germany. E-mail: sunt@uni-muenster.de; Fax: (+49)251-83-33602; Tel: (+49)251-83-63841*
[d]*Beijing Institute of Transfusion Medicine, Beijing, 100850, P. R. China*
† Electronic supplementary information (ESI) available: Experimental details; characterization of monomers and polymer films; control experiment for cell culture. See DOI: 10.1039/c0sm00151a
‡ H. Gan and X. Wang contributed equally to this work.

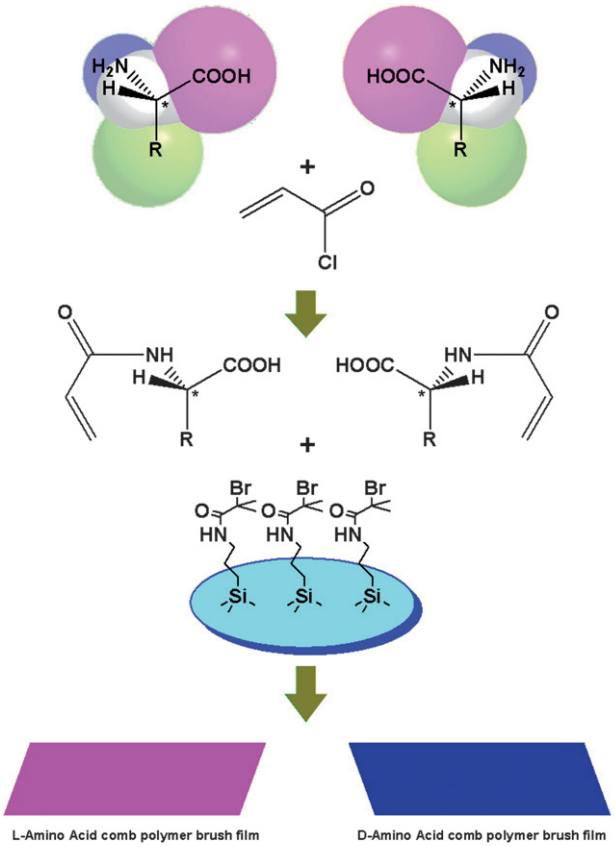

Scheme 1 Synthesis protocol for the chiral polymer brush films. The first step is to synthesize the chiral monomer of L(D)-acryloylated amino acids through the reaction between amino acids and acryloyl chloride. The second step is to obtain the chiral polymer brush film by the surface initiated atom transfer radical polymerization method.

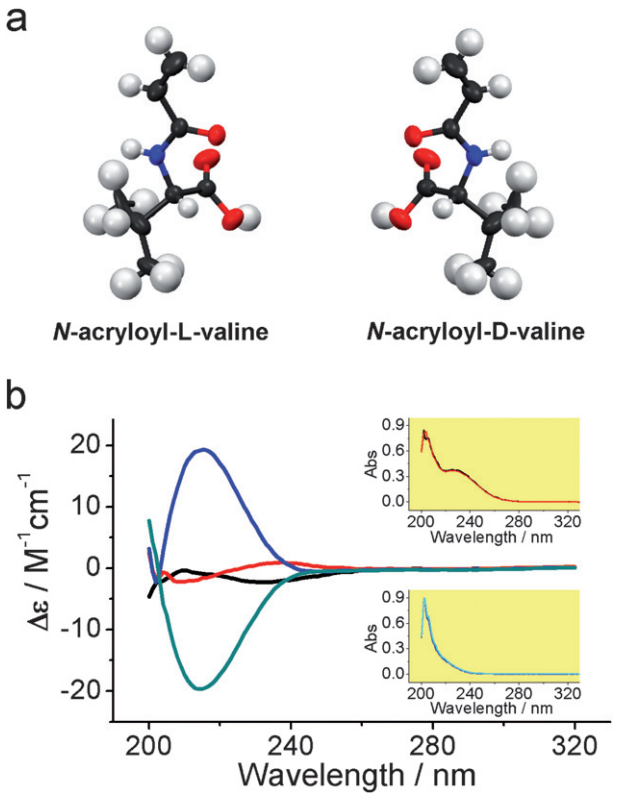

Fig. 1 (a) Steric configurations of the *N*-acryloyl-L(D)-valine monomers obtained from the crystal analysis data. (b) CD spectra for L(D)-PV polymers and the corresponding monomers. Black: *N*-acryloyl-L-valine monomer; red: *N*-acryloyl-D-valine monomer; blue: L-PV polymer; cyan: D-PV polymer. The insets are the UV-vis spectra for the polymers (lower) and the monomers (upper), in which the absorbance intensity at 202 nm peak for –COOH groups were used to characterize their effective concentrations. The perfect mirror-image relationship between the CD spectra for the L(D)-PV polymers and the much higher optical rotation activity compared with the monomers indicate that the chirality was preserved very well after the polymerization process. X-Ray photoelectron spectrum study (see ESI†) shows that the films are identical in chemical compositions, which is verified by coincide between their UV-vis spectra.

influencing their bioactivities and the relevant bioprocesses. Based on this reason, we selected the amino acid enantiomers as the chiral units in the design of the polymer brushes,[22] which contain an achiral polyacryloyl backbone, and the amino acid units are linked to the backbone in a comb teeth style through the amide bonds. For preparation (as schematically shown in Scheme 1), the film was grafted onto the silicon wafer *via* the surface initiated atom transfer radical polymerization (ATRP) method[23] starting from monomers of L(D)-acryloylated amino acids. Since there are more than 20 natural amino acid species, we chose the L(D)-valine based polymer brushes (denoted as L-PV and D-PV, respectively) as a representative for the studies in the following.

The *N*-acryloyl-L(D)-valine monomers that were used for the polymerization exhibit excellent crystallinity and the 3-dimensional molecular structures obtained from the crystal analysis data (for details, see ESI†) are shown in Fig. 1a. It indicates a very high chiral purity for the L(D)-isomers. Fig. 1b shows the circular dichroism (CD) spectra for the monomers and the corresponding L-PV and D-PV polymers at the same effective concentration (as indicated by the UV absorbance intensities for –COOH groups, see insets of Fig. 1b). The perfect mirror image relationship for the curves and the much larger $\Delta\varepsilon$ values for the polymers than the monomers prove that the chirality was well preserved after the ATRP process and the optical rotation activity was largely enhanced by forming polymers.

The atomic force spectroscopy (AFM) and ellipsometry studies show that the as-prepared polymer brush films are identical in surface morphology (Fig. 2a and b), and that the films are quite uniform and smooth (roughness less than 2 nm) in a large scale range (at least hundreds of micrometres, as indicated by the ellipsometry study). The film thickness is in a range of 10–14 nm for both D- and L-films. Wettability measurements show that they are hydrophilic with contact angles of about 52 ± 2°. X-ray photoelectron spectroscopy (XPS) proves that the chemical compositions of the two films are also the same. These results reveal that the L(D)-PV films are identical in both the physical and chemical properties, except for the opposite chirality.

We first used a fibroblast-like cell line—COS-7 cells to investigate the cell behaviour on the chiral polymer brush films (for the cell culture experiments, each experiment has been repeated for at least 6 times, and all data provided below were the statistic

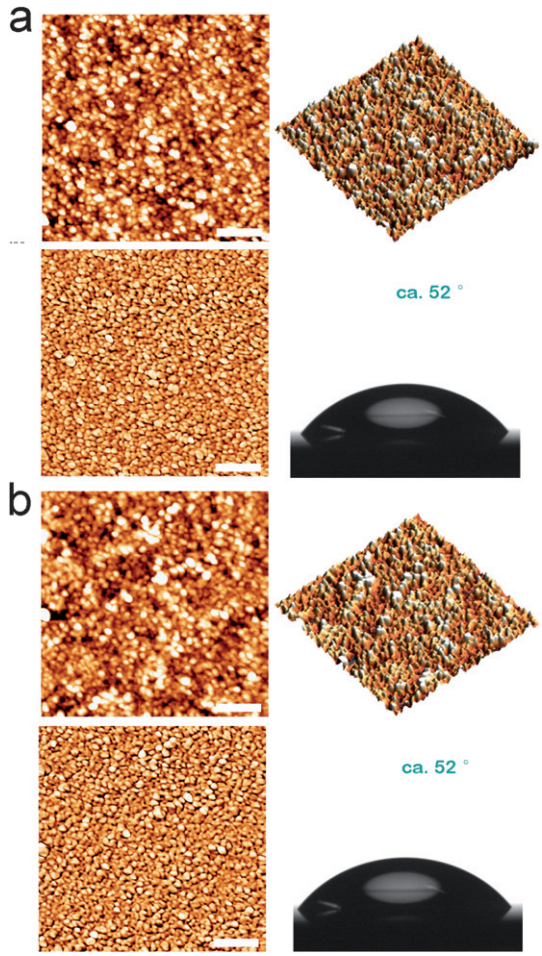

Fig. 2 Film property characterization of the L-PV (a) and D-PV films (b) by AFM and wettability studies. Upper left: 2-dimensional AFM image; upper right: 3-dimensional AFM image; lower left: corresponding phase image; lower right: contact angle (CA) measurement shows that the films are hydrophilic with same CAs of about 52°. Scale bar: 200 nm.

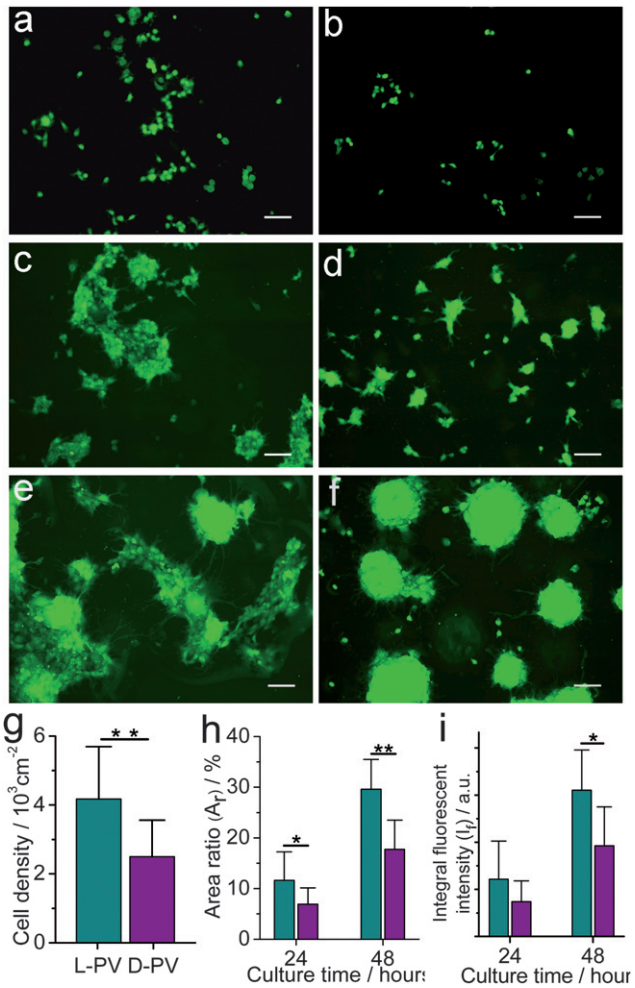

Fig. 3 Cell culture experiments for COS-7 cells on the chiral polymer brush films. (a–f) Typical fluorescent images on L-PV (a, c, e) and D-PV films (b, d, f) at different incubation stages. (a, b) 1 h; (c, d) 24 h; (e, f) 48 h. (g) Cell counting results for 1 h of incubation. (h) Surface area ratios (A_r) occupied by cells after 24 and 48 h of incubation. (i) Integral fluorescent intensities (I_f, by arbitrary units (a.u.)) for the cell occupied areas on images after 24 and 48 h of incubation. The data in (h) and (i) were obtained by the Volocity (Improvision) image processing system. For the statistic analysis of these data, one asterisk means $P < 0.05$ for the t-test; while double asterisks mean $P < 0.01$. Cyan: L-PV film; purple: D-PV film. Scale bars for (a–f) are 100 μm.

results for all experiments, see ESI† for details). Fig. 3 shows typical fluorescent microscopic images after different periods of cell incubation. For 10 min of incubation, only a small amount of cells were attached onto the films and all cells were distributed separately with round morphology. With the elongation of the incubation time, more and more cells were adhered onto the surface, in which a significant difference could be observed on L- and D-PV films. As shown in Fig. 3a and b for 1 h of incubation, the cell density on the L-PV film (average of 4.17×10^3 cm^{-2}) is apparently higher (t-test: $P < 0.01$, Fig. 3g) than that on the D-PV film (average of 2.50×10^3 cm^{-2}).

For longer incubation time, the cell density on surfaces increased further. At the same time, the difference between the L(D)-PV films exhibited some new aspects, which reflected not only on the cell quantity, but also on cell morphology and configuration. Fig. 3c and d show the results of 24 h. On the L-PV film, the cells spread and connected to each other to form large interlinked clusters.

However, on the D-PV film, the spreading extent was much lower and the cells preferred much more to remain isolated stacks. The SEM images (Fig. 4) show the difference on the two films with more details, in which the cell connection on the L-PV film (Fig. 4a) can be clearly observed, while the piling-up cells on the D-PV film (Fig. 4b) exhibit roughly round morphology. Because it is difficult to determine the cell quantity accurately due to the complicated cell spreading and overlapping, we used two parameters to characterize quantitatively the cell behaviour for long incubation time, which were obtained through analyzing the fluorescent images by the Volocity (Improvision) and Photoshop CS (Adobe) software.[24,25] The first is the area ratio of the surface (defined as A_r) occupied by cells, describing the two-dimensional cell growth on the substrate. The second is the integral fluorescent intensity (defined as I_f) of the image for the cell covered regions. It gives a three-dimensional expression for the overall cell quantity and volume on the surface. As shown in Fig. 3h, the average value of A_r on the L-PV film is about 11.61%, which is

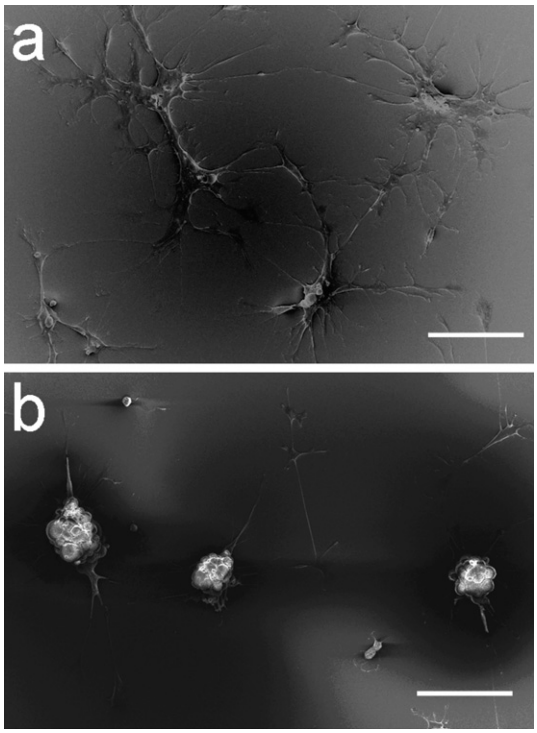

Fig. 4 SEM images for cell (COS-7) morphology on chiral polymer brush films after 24 h of incubation. (a) L-PV film. (b) D-PV film. Scale bar: 100 μm.

much larger (t-test: $P < 0.05$) than that on the D-PV film (averagely 6.90%). Simultaneously, the average I_f value (Fig. 3i) on the L-PV film seems to be higher than that on the D-PV film, although significance is not shown here.

The difference became more significant when the incubation time was prolonged to 48 h. As shown in Fig. 3e, the two-dimensional growth, spreading and connection of cells made the cells to form large and highly interconnected two-dimensional assemblies on the L-PV film. However, on the D-PV film, it seems that the cells did not prefer the surface and could not form effective connections with each other through the guidance of the substrate, while instead, the cells preferred to grow on the top of other cells and form the isolated large clusters. Accordingly, the fluorescent intensity of a single large cluster on the D-VP film is much higher (revealing a thicker cell layer) than the cell assemblies on the L-VP film. It shows that the formation of the large clusters on the D-VP film is mainly due to the cell proliferation, but not the cell spreading and connection. For the quantitative analysis (Fig. 3h and i), L-PV film also exhibited much larger average A_r (t-test, $P < 0.01$) and I_f values (t-test, $P < 0.05$) than the D-PV film. These data clearly demonstrate the much different growth and assembly tendencies of COS-7 cells on the two chiral surfaces: on the L surface, the cells prefer to grow and assemble along the two-dimensional surface directions; while on the D surface, the cells would mainly proliferate three-dimensionally. Such different growth and assembly tendencies reveal that the L-PV film has much higher cytocompatibility than the D-VP film.

The above results disclose the different behaviour of COS-7 cells on the L- and D-PV films at various incubation stages. For the short incubation stage, the cells exhibited much different

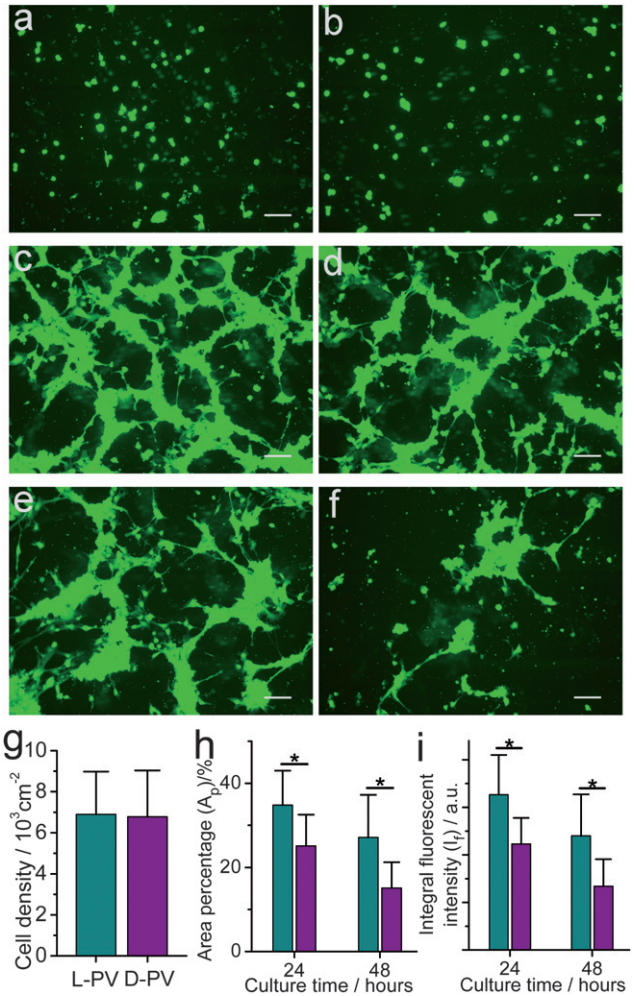

Fig. 5 Cell culture experiments for bEnd.3 cells on the chiral polymer brush films. (a–f) Typical fluorescent images on L-PV (a, c, e) and D-PV films (b, d, f) at different incubation stages. (a, b) 1 h; (c, d) 24 h; (e, f) 48 h. (g) Cell counting results for 1 h of incubation. (h) Surface area ratios (A_r) occupied by cells after 24 and 48 h of incubation. (i) Integral fluorescent intensities (I_f) for the cell occupied areas on images after 24 and 48 h of incubation. The data in (h) and (i) were obtained by the Volocity (Improvision) image processing system. For the statistic analysis of these data, one asterisk means $P < 0.05$ for the t-test. Cyan: L-PV film; purple: D-PV film. Scale bars are all 100 μm.

attachment and adhesion behaviours on the chiral substrates. For longer incubation stages (*e.g.* 24 and 48 h), since the attachment process normally occurs in a relative short time scale (*e.g.* 1 h) and those have failed to adhere onto the substrate will initiate the apoptosis process,[26,27] the different assembly and growth behaviours of the cells are mainly related to the divergence in subsequent cellular events like proliferation, differentiation and migration, apoptosis, and other processes, *e.g.* ECM reconstruction.[28] In order to get more information regarding the cytocompatibility of the L- and D- films, we also used a different cell type—endothelial cells (bEnd.3) in our cell culture experiments. There was no difference (t-test, $P \gg 0.05$, Fig. 5g) between cell quantities on the L(D)-PV films at 1 h (Fig. 5a and b). However, at 24 h (Fig. 5c and d), the cells have spread and formed contacts resulting in a highly linked two-dimensional

network, and the difference between the L(D)-PV films became distinct, in which the L film has higher average A_r and I_f values than the D film (t-test, $P < 0.05$, see Fig. 5h and i). After incubation for 48 h (Fig. 5e and f), the cell quantity decreased with obvious reductions in the A_r and I_f values compared with 24 h on both films. Interestingly, the decrease was more substantial on the D-PV film than on the L-PV film, resulting in significant differences (t-test, $P < 0.05$) for A_r and I_f values (Fig. 5h and i) between them. The reduction in cell number is caused by the apoptotic or necrotic cell death. Since dead cells will normally leave the surface,[29] the lower decrease of the surface coverage level on the L film indicates that the cells may have a smaller apoptosis and necrosis rate than those on the D film. This also points to a clear difference in the cytocompatibility between the two chiral surfaces.

Thus it can be inferred that the cells can sense the steric configurations of molecules on substrates and respond differentially according to their chirality, although the other surface chemical and physical properties remain the same. The stereochemistry of the substrate can greatly influence the interaction between cells and the polymer films and thereby critical cellular functions including adhesion, spreading, growth, assembly and apoptosis. Similarly, Hanein *et al.*[11] also reported the differential adhesion behaviour of epithelial cells on enantiomorphous crystal faces. Together with our previous report of the stereospecific adhesion and activation of immune cells on the chiral self-assembly surfaces, it shows that this effect is not unique, but may be generally applicable for different materials and cells. In the *in vivo* applications of biomaterials, this behaviour determines in a large extent their performance. Therefore, the chiral effect implies a novel strategy for the design of high-performance biomaterials and devices, which is much different from, but well complementary to the conventional methods based on surface wettability, chemical compositions, topographic structures, *etc*. The mechanisms underlying the differential cell behaviour on chiral films should be related to the stereoselective recognition and binding between the chiral moieties of the polymer brush films and cells, which would result in both complex intracellular signalling cascades and physical or chemical interactions[30,31] of extracellular components with cell surface proteins.[32] The mechanism study may also bring much interesting insight into the chiral preference of biomolecules in nature, and remains an important task of our future research.

Conclusions

In conclusion, we developed a novel chiral polymer brush film system and report that stereochemistry of the polymer film greatly influences cellular behaviour on a substrate, including adhesion, spreading, assembly, proliferation, and apoptosis. Due to the much better growth of cells on the L film than that on the D film, it indicates that the L configuration of the surface is more beneficial for the improvement of the cytocompatibility of materials. These results imply a novel strategy for the design of new generation of biomaterials and devices based on the chiral effect. Further studies are still underway to investigate this effect in the *in vivo* environment and explore its underlying molecular and biochemical mechanisms, which may help to elucidate the chiral preference in biosystems.

Acknowledgements

We thank for the Alexander von Humboldt (AvH) Foundation and the Federal Ministry of Education and Research of Germany (BMBF) for partial financial support (Sofja Kovalevskaja Award project).

References

1 N. A. Peppas and R. Langer, *Science*, 1994, **263**, 1715–1720.
2 R. Langer and D. Tirrel, *Nature*, 2004, **428**, 487–492.
3 R. O. Hynes, *Science*, 2009, **326**, 1216–1219.
4 T. Sun, H. Tan, D. Han, Q. Fu and L. Jiang, *Small*, 2005, **1**, 959–963.
5 H. Zhang, G. M. Annich, J. Miskulin, K. Stankiewicz, K. Osterholzer, S. I. Merz, R. H. Bartlett and M. E. Meyerhoff, *J. Am. Chem. Soc.*, 2003, **125**, 5015–5024.
6 V. Mironov, V. Kasyanov and R. R. Markwald, *Trends Biotechnol.*, 2008, **26**, 338–344.
7 L. Chen, M. Liu, H. Bai, P. Chen, F. Xia, D. Han and L. Jiang, *J. Am. Chem. Soc.*, 2009, **131**, 10467–10472.
8 R. M. Hazen and D. S. Sholl, *Nat. Mater.*, 2003, **2**, 367–374.
9 R. Corradini, S. Sforza, T. Tedeschi and R. Marchelli, *Chirality*, 2007, **19**, 269–294.
10 R. Bentley, *Chem. Soc. Rev.*, 2005, **34**, 609–624.
11 D. Hanein, B. Geiger and L. Addadi, *Science*, 1994, **263**, 1413–1416.
12 T. Sun, D. Han, K. Riehemann, L. Chi and H. Fuchs, *J. Am. Chem. Soc.*, 2007, **129**, 1496–1497.
13 C. J. Buchko, L. C. Chen, Y. Shen and D. C. Martin, *Polymer*, 1999, **40**, 7397–7407.
14 T. Moro, Y. Takatori, K. Ishihara, T. Konno, Y. Takigawa, T. Matsushita, U. Chung, K. Nakamura and H. Kawaguchi, *Nat. Mater.*, 2004, **3**, 829–836.
15 S. I. Yusa, K. Fukuda, T. Yamamoto, K. Ishihara and Y. Morishima, *Biomacromolecules*, 2005, **6**, 663–670.
16 J.-F. Lutz, H. G. Borner and K. Weichenhan, *Macromolecules*, 2006, **39**, 6376–6383.
17 S. Edmondson, V. L. Osborne and W. T. S. Huck, *Chem. Soc. Rev.*, 2004, **33**, 14–22.
18 T. Sun, G. Wang, L. Feng, B. Liu, Y. Ma, L. Jiang and D. Zhu, *Angew. Chem., Int. Ed.*, 2004, **43**, 357–360.
19 W. A. Petka, J. L. Harden, K. P. McGrath, D. Wirtz and D. A. Tirrell, *Science*, 1998, **281**, 389–392.
20 S. Mitragotri and J. Lahann, *Nat. Mater.*, 2009, **8**, 15–23.
21 J. Chelaflores, *Chirality*, 1994, **6**, 165–168.
22 H. Mori, H. Iwaya, A. Nagai and T. Endo, *Chem. Commun.*, 2005, 4872–4874.
23 D. M. Jones and W. T. S. Huck, *Adv. Mater.*, 2001, **13**, 1256–1259.
24 R. Benedito, C. Roca, I. Sörensen, S. Adams, A. Gossler, M. Fruttiger and R. H. Adams, *Cell*, 2009, **137**, 1124–1135.
25 A. J. Hand, T. Sun, D. C. Barber, D. R. Hose and S. Macneil, *J. Microsc.*, 2009, **234**, 62–79.
26 C. S. Chen, M. Mrksich, S. Huang, G. M. Whitesides and D. E. Ingber, *Science*, 1997, **276**, 1425–1428.
27 K. Webb, V. Hlady and P. A. Tresco, *J. Biomed. Mater. Res.*, 2000, **49**, 362–368.
28 E. A. Silva and D. J. Mooney, *Curr. Top. Dev. Biol.*, 2004, **64**, 181–205.
29 A. P. Acharya, N. V. Dolgova, M. J. Clare-Salzler and B. G. Koselowsky, *Biomaterials*, 2008, **29**, 4736–4750.
30 K. Tang, H. Gan, Y. Li, L. Chi, T. Sun and H. Fuchs, *J. Am. Chem. Soc.*, 2008, **130**, 11284–11285.
31 H. Gan, K. Tang, T. Sun, M. Hirtz, Y. Li, L. Chi, S. Butz and H. Fuchs, *Angew. Chem., Int. Ed.*, 2009, **48**, 5282–5286.
32 V. Vogel and M. Sheetz, *Nat. Rev. Mol. Cell Bio.*, 2006, **7**, 265–275.